ANNALES
UNIVERSITATIS MARIAE CURIE-SKLODOWSKA
LUBLIN — POLONIA
VOL. XLVI/XLVII, 37 SECTIO AAA 1991/1992

Saha Institute of Nuclear Physics, Sector-1, Block-AF, Bidhannagar, Calcutta (India)

P. RAJASEKAR, P. CHAKRABORTY

SIMS in the Perspectives of Some High-T_c Superconducting Materials

INTRODUCTION

Secondary ion mass spectrometry, commonly known as SIMS, is a technique which utilizes a focused beam of low energy ions or neutral particles, mostly of inert gases, in general, in some keV range of energy, for bombardment of a surface of a solid or liquid, followed by the subsequent mass analysis and detection of the sputtered particles (atoms or molecules) which are in the ionized state. The impact of a primary particle on a surface causes a transfer of energy and momentum to a limited area, around the point of particle contact, giving rise to the phenomena of secondary emission which include the electron and photon emission and the emission of surface particles (sputtering), atomic and/or molecular, in a charged (both positive and negative) or neutral state. Some of these ejected particles are possibly in the excited states also. Therefore, the process of secondary ion emission is essentially a process of sputtering, coupled with the ionization. Fig. 1 shows schematically the principle of SIMS.

Since all secondary ions mostly originate from the uppermost atomic layers of the bombarded surface, from the elemental analysis of these secondary ions or in other words, by recording e/m spectrum of the emitted secondary ions, one can get a direct information about the chemical composition of the sample surface or of the uppermost layers of the target sample. Therefore, if the sputtering yield (number of total emitted particles per incident ion) and the ionization probability of the emitted species are known direct information about the lateral elemental distribution across the sample surface can be extracted. This results in one of the most important features of SIMS — its surface sensitivity. However, this concerns the static SIMS where the surface composition and microstructure remain practically unaffected by the primary ion current densities. For example, for an ion current density of 10^{-9} A/cm^2 a surface monolayer lasts for some orders of several hours [1]. Static SIMS has been successfully applied for the determination of the chemical

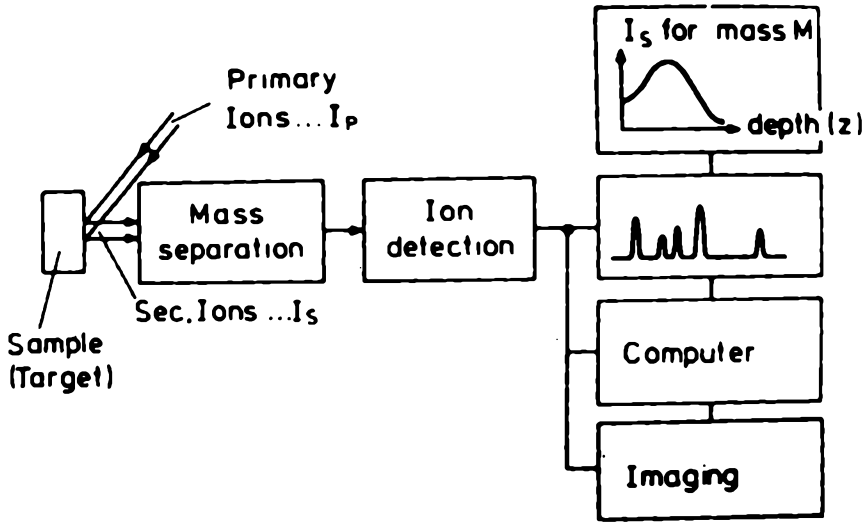

Fig. 1. Principle of SIMS (after Benninghoven *et al.* [1])

composition of the uppermost monolayer of metals, alloys, semiconductors, organic materials and so on. Static SIMS may be considered as complementary to the other surface analytical techniques, such as AES (Auger Electron Spectroscopy), XPS (X-ray Photoelectron Spectroscopy), ISS (Ion Scattering Spectrometry), TDMS (Thermal Desorption Mass Spectroscopy), etc.

On the other hand, dynamic SIMS makes use of high primary ion current densities up to some amp/cm^2, causing thereby a continuous removal of surface layers. Therefore, continuous monitoring of a secondary ion signal as a function of time, calibrated against depth, provides depth distribution of the particular species within the bulk material of the sample. By using dynamic SIMS, depth profiling of elemental concentration can be achieved with high sensitivity down to ppb range. Dynamic SIMS with a focused scanning ion beam allows a three--dimensional analysis of the sample (imaging). This technique has been found to be very sensitive for analysis of semiconductors and integrated circuits.

Depending on the analytical application of the SIMS technique, various kinds of mass spectrometers are used for e/m separation. The first SIMS instruments were equipped with the sector-type magnetic mass spectrometers. Later on, double-focussing sector-field instruments (energy and momentum separation) were employed because of their inherent high sensitivity. But owing to the broad energy spectrum and the large solid angle of emission of the secondary sputtered ions from the target, complicated ion-optical problems had to be overcome in separator design to minimize the loss in intensity of secondary ions. In this respect, quadrupole mass analyzers have proved to be very successful for their inherent large accep-

tance and wide energy band pass. Moreover, static SIMS needs an e/m analyzer with a high overall transmission for ions originating from a relatively large area. This is the reason why quadruple instruments have been so widely applied, especially in the field of static SIMS. Two other types of mass analyser, such as time of flight and ion-cyclotron mass analyzers are also frequently used [2,3] for high SIMS performance where detection of elements, present in extremely low concentrations in a sample, is required, in addition to the requirement of high lateral resolution. Both these instruments are successfully used in static as well as in dynamic SIMS. A comprehensive up-to-date coverage on SIMS instruments has been given by Benninghoven *et al.* [1].

The excellent micro-analytical capabilities of the SIMS technique have been enormously exploited in a wide spectrum of scientific and technical areas. Out of the wide range of applications [1], the majority of SIMS applications are, by far, concerned with electronic materials and devices. Very recently, special efforts have been focused in the field of oxide-base superconductors soon after the discovery [4] of high-T_c superconductivity (HTSC) in 1986 in the new rare-earth copper oxide systems, like La-Ba-Cu-O. Since then, considerable progress has been made towards producing a variety of oxide materials of improved sample quality, in general, and single crystal, in particular, that superconduct at higher and higher transition temperatures (T_c). Structures of these various high-T_c superconducting ceramic compounds in all their complexities are also becoming more and more understandable following extensive characterizations of these compounds by various techniques. Simultaneously, enormous amount of theoretical approaches on this topic represents a consolidated activities on the search for newer and better mechanisms to account for such high transition temperatures and a necessary stage in the comprehension of the various experimental results obtained and thus, in deciding on the course of further investigations.

Among the different characterization techniques, the most widely studied in this field so far, are the various spectroscopic methods [5]. To mention, few recent comprehensive reviews [6,7] have been dedicated to the critical assessment of the various studies that were conducted in the period 1987 to early 1991 in the field of *x-uv* and photo-electron spectroscopy of high-T_c superconductors. Both these reviews have discussed essentially on the X-ray and photoelectron spectra-based analysis of electronic structure and pairing mechanisms of high-T_c superconductors (HTSCs). The general concept that the important role in producing high values of T_c is played by the density of states on E_f (Fermi level), as is consistent with both electron-phonon and purely electron mechanism of HTSCs, was found to be confirmed by the above studies [6,7].

A critical review [8] of few recent experiments in the field of cuprate superconductors has appeared where the following aspects, like carrier (charge) response and spin excitations in the normal state, density of states near the Fermi level and mass enhancements (effective mass of carriers is four times as high as that of a free electron, estimated from various experimental probes) etc. have been discussed. These aspects form the basis to the understanding of the unique properties of the layered cuprate superconducting compounds.

The wide range of experimental studies in the field of high-T_c superconductivity, reported so far, have practically excluded SIMS. This is possibly because of the fact that very few as well as unsystematic works in this field have been undertaken that have made use of this particular surface analytical technique.

In the present article, an attempt has been made to illustrate the various SIMS studies, which are so far available for the investigation of oxide-based superconducting materials.

SECONDARY ION SPECTRA AND STRUCTURAL ASPECTS

Most probably, the first paper in this area was reported by Allen and Brown [9], who investigated the surface properties of fully oxygenated superconducting compound $Y_1Ba_2Cu_3O_7$ of orthorhombic structure, using liquid gallium ion-induced secondary ion mass spectrometry. They examined a freshly prepared sample as well as the same after exposure to atmosphere. Their results in the latter case revealed that surface reactions took place with moisture as well as with some contaminants, like hydrocarbons. Those surface layers were readily sputtered away due to ion bombardment, although the presence of yttrium and barium hydroxides was apparent in the SIMS spectra [9].

The nature and origin of the foreign impurities, such as oxides and hydroxides of barium, yttrium, copper, etc., regardless of whether they are formed as a result of imperfections of the various methods of producing HTSC (i.e. bulk impurities), or because of the formation of 'surface' compounds under the action of reactive medium, like moisture etc. were determined by Palatnik and Klimovskii [10]. They measured the intensity ratio of the emitted oxides and hydroxides of Y, Ba, Cu, etc. in case of HTSC for two different values of primary beam current density and observed that for barium and copper this ratio remained virtually constant for lower as well as higher beam current density. This signifies that hydroxides of barium and copper in the YBCO sample were 'bulk impurity' compounds [10], since their intensities changed in the same proportion with the changes in the intensities of the corresponding oxides as the beam current density was varied. Whereas for yttrium, this ratio was found to increase considerably for the higher beam current density. In this case the intensity of YOH^+ did not increase with the increase of beam current indicating the origin of YOH^+ as from the YBCO surface [10].

Secondary emission of individual ionic species from various high-T_c materials has been explained in the light of their known crystallographic structures [10–13]. While observing the $BaOH^+$ emission from the surfaces of orthorhombic $Y_1Ba_2Cu_3O_{7-x}$ (YBCO) as well as from non-superconducting tetragonal $Y_1Ba_2Cu_3O_6$ compounds after surface reaction with moisture in both the cases [11], a comparatively lower emission of $BaOH^+$ signal for YBCO as well as for $Y_1Ba_2Cu_3O_6$ samples [11] showed the deeper penetration of water molecules as well as their interaction in a larger amount in case of tetragonal structure (annealed sample) than in the case of orthorhombic structure. The reason was explained to be due to the fact that Cu–O planes (basal planes) in the tetragonal structure, being devoid of oxygen

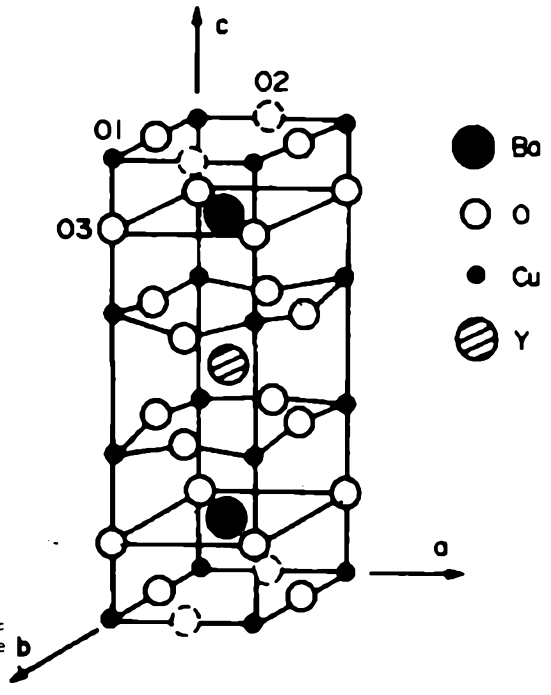

Fig. 2. Orthorhombic structure of high-T_c superconducting $Y_1Ba_2Cu_3O_{7-x}$ lattice (after Chenakin [11])

(unlike in the case of basal planes of orthorhombic $Y_1Ba_2Cu_3O_{7-x}$, as shown in Fig. 2), might be occupied with OH (hydroxyl) to a larger extent [11].

The SIMS spectra of a freshly prepared YBCO (shown in Fig. 3) shows the peaks due to the metal monoxide (MO^+) ions, except in the case of copper oxide [9]. The intensity of sputtered MO^+ ions relative to that of M^+, was found to be a logarithmic function of its dissociation energy [9] which suggests that as the dissociation energy of a metal oxide decreases, its formation probability also decreases in the secondary emission process. Since CuO has extremely low dissociation energy (0.71 eV), the production of CuO^+ is thermodynamically unfavourable in the sputtering process. This is the reason why peaks of CuO^+ ions were not found in the SIMS spectra of YBCO and insulating La_2CuO_4 materials [9]. The absence of CuO^+ peaks in the SIMS spectra of YBCO [10,12], $(Bi,Pb)_2Sr_2Ca_2Cu_3O_{10+\delta}$ or (Bi,Pb)-2223 [12] and also of various oxides of copper [14] has also been confirmed by Rajasekar *et al.* in their recent experiments.

In $Y_1Ba_2Cu_3O_{7-x}$, there are continuous chains of Cu and O-atoms along b--axis and only Cu atoms along a-axis in basal planes (Fig. 2). Owing to being such direct short-range Cu-Cu bonding in the above structure, 'as such' emission of Cu_2^+ secondary ions is quite probable [11,12]. It can be noted that for the annealed YBCO compounds with tetragonal structure, e.g. for $Y_1Ba_2Cu_3O_6$ and also for $Er_1Ba_2Cu_3O_6$ [11], the emission of Cu_2^+ was always found to be slightly higher ($Cu_2^+/Cu^+ \sim 0.16$) than in the case of $Y_1Ba_2Cu_3O_{7-x}$ ($Cu_2^+/Cu^+ \sim 0.12$). It was attributed to the fact that in a tetragonal lattice there are no oxygen atoms along

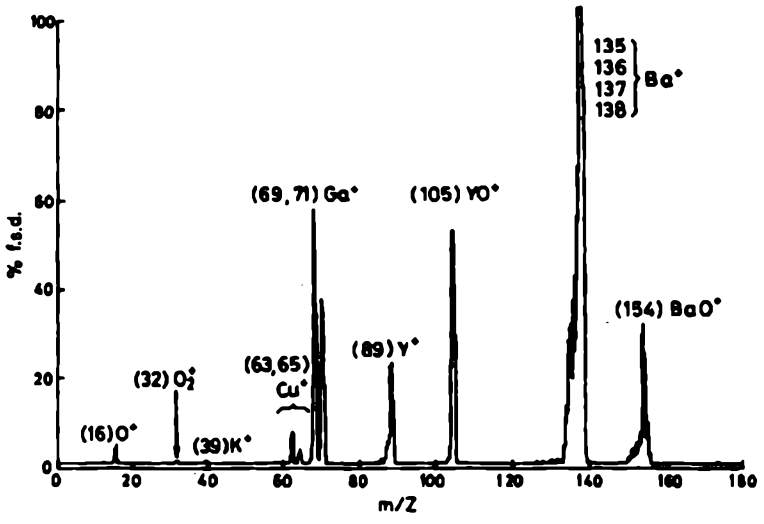

Fig. 3. SIMS spectrum of $Y_1Ba_2Cu_3O_{7-x}$ (after Allen and Brown [9])

the b-axis in the basal planes and full copper planes are formed, giving rise to more emission of Cu_2^+ than for HTSC. However, in the (Bi,Pb)-2223 structure (Fig. 4) there are no such direct Cu-Cu bonding in any of the lattice planes, all Cu-atoms being present in various Co-O planes. Even for such a structure, emission of Cu_2^+ dimers was found to be possible with its intensity relative to that of Cu^+ being almost comparable with that in the YBCO situation [12]. Therefore, it was argued that Cu_2^+ emission was possible either from three Cu-atom segments existing along c-direction or from CuO_2 planes of the (Bi,Pb)-2223 structure. Weak binding between Cu and O atoms in a CuO complex may lead to the dissociation into individual species of Cu and O under primary ion bombardment. Subsequent recombinations into Cu_2 and O_2 dimers could thus explain the observation of the corresponding ionic dimers in the case of (Bi,Pb)-2223 structure. Such a process of dimer formation from CuO_2 planes and CuO chains of YBCO structure might be possible, in addition to the more significant contribution of 'as such' emission of Cu_2^+ from Cu-Cu chains, as discussed earlier. Similarly, observation of Ca_2^+ signal in case of (Bi,Pb)-2223 structure [12] can be explained as the emission of Ca_2^+ ions from continuous planes containing Ca atoms only (Fig. 4).

The intensity of YO^+ secondary ions was found to be comparable with that of Y^+ for YBCO structure (Fig. 3). It is believed that as in the case of dimers, YO^+ molecular ions are also emitted 'as such'. Such Y-O blocks comprising any Y-atoms and any of the O-atoms of the neighbouring CuO_2 planes exist in the structure. In fact, the significantly high bond-dissociation energy of YO^+ ions [(7.8 ± 1.0) eV, as measured by Allen and Brown [9], should favour 'as such' emission of YO^+

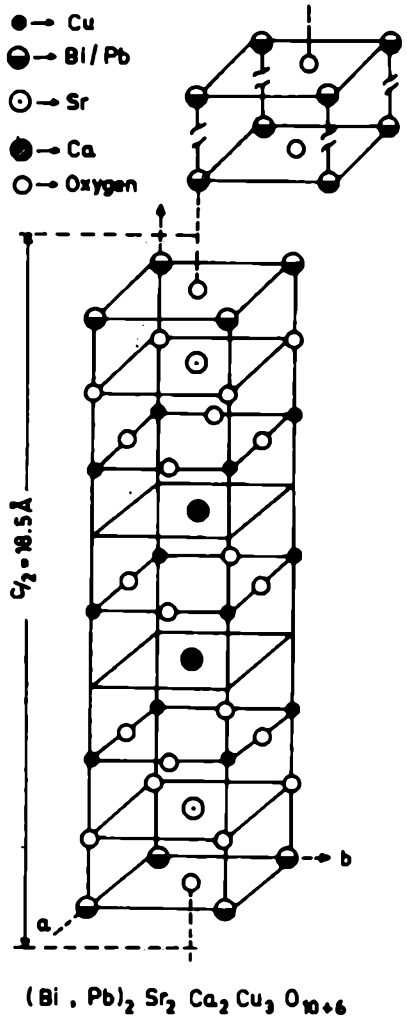

Fig. 4. Structure of high-T_c superconducting $(Bi,Pb)_2Sr_2Ca_2Cu_3O_{10+\delta}$ lattice (after Rajasekar *et al.* [12])

ions. Emission of Y^+ can take place from the Y-planes of the structure, and also by the dissociation of the YO complexes, Y^+ ions originating due to the latter process are likely to carry a part of the high energy of dissociation of the YO-complex. This should explain why the peak of the energy distribution of Y^+ secondary ions was found to be shifted towards higher value compared with that for other secondary ions, like Ba^+, Cu^+, etc. emitted from the same YBCO structure [15]. As seen in Fig. 2, there are no short-range neighbouring atoms like Y-Cu, Ba-Cu, Y-Ba, etc. in the YBCO lattice and therefore, such complexes are usually absent in the SIMS spectra of the same structure. However, these metallic atoms, present in the lattice, are strongly bound through oxygen and this strong oxygen bond in the atomic chains increases the probability of the direct emission of the complexes, like $(Ba\ O\ Cu)^+$, $(Y\ O\ Ba\ O\ )^+$, $(Ba\ O\ Cu\ Y)^+$ etc. [16]. Emission of such ionic complexes with intensities comparatively higher than those of atomic ions have indeed been observed by Chenakin [11].

BINDING SITUATIONS IN YBCO STRUCTURE

The energy spectra of various secondary ions emitted from HTSC reflects the binding situation in the structure. Let us examine the energy spectra of secondary ions Y^+, YO^+, Ba^+, Cu^+, O^+ etc., emitted from a YBCO structure and that of Y^+ and YO^+ from an oxygen covered metallic Y [11] (Fig. 5). It may be seen from the figure that the energy distribution of Y^+ in the case of YBCO is characterized by the highest values of the most probable energy $E_m = (24 \pm 3)$ eV and FWHM$\sim$52 eV, which exceed significantly the corresponding parameters for other ionic species not only in the case of YBCO but also, of Y. Supposing that the declining part of the energy distribution (beyond the region of maximum) of sputtered atoms emitted from those samples follows the well-known dependence $N(E) \sim E^{-2}$, the ionization probability $\alpha^+(E)$ for Y-atoms was estimated from the experimental secondary ion spectra $N^+(E)$ [11]. For the high energy tail of the distributions, it turned out to be a power-law dependence, i.e. $\alpha^+(E)\ \alpha E^n$, where $n \simeq 1$ for Y^+, emitted from both YBCO and oxygen-covered yttrium (Fig. 5). This is in good agreement with the power-law dependence of α^+ (where $n \simeq 1.1$) found for oxygen-covered beryllium [17]. Then using the value of most probable energy E_m of the distribution $N^+(E)$ in the relation, $E_m = E_b(n+1)(2-n)$ (ref. 18), where E_b is the surface binding energy of the atoms, the surface binding energy of Y-atoms was found to be $\sim$ 12 and 3.9 eV for the YBCO and metallic yttrium, respectively [11]. Although, another proposal was made by Kosyachkov [19], according to whom, the peak energy of sputtered ions, i.e. E_m, of some particular species is approximately equal to the surface binding energy E_b of that species in the metal oxide. According to this suggestion, the surface binding energy E_b of Y-atoms in the YBCO structure becomes 24 eV instead of 12 eV, as the observed peak energy of sputtered Y--ions from the same structure lies around 24 eV, as seen from the energy spectra [11,19]. This relation (i.e. $E_m \simeq E_b$ was found to be satisfactory so as to give the best agreement between the calculated and experimentally measured ionization probabilities of the atoms, sputtered from a number of carbides [20] and was also

found to be useful for explaining the appearance of double peaking, observed in the energy distributions of some secondary ions emitted from YBCO structures [19]. Specifically, these two peaks were distinctly visible in the energy spectra of Ba^+ and BaO^+. Since the low energy peak disappeared after vacuum annealing, this was attributed to the initial state of the ceramic only [19].

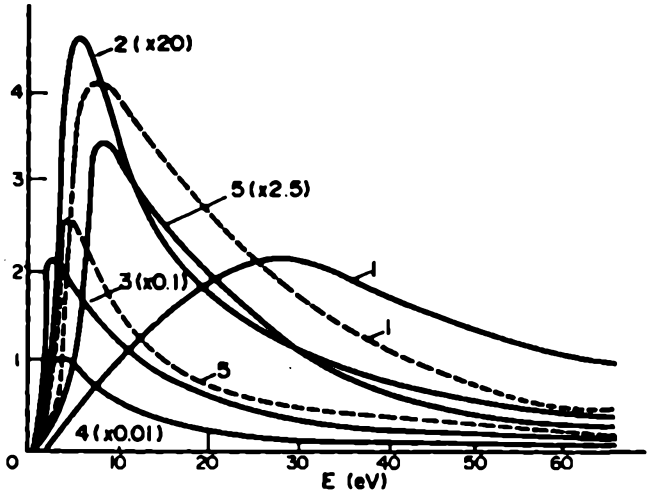

Fig. 5. Energy spectra of secondary ions Y^+ (1), Ba^+ (2), Cu^+ (3), O^+ (4), YO^+ (5), emitted from $Y_1Ba_2Cu_3O_{7-x}$ (solid line) and oxygen-covered yttrium (dashed line) (after Chenakin [11])

High binding energy of Y atoms in the YBCO was found to be consistent with the measurement of the relative intensity of YO^+ to Y^+ from oxygen-covered yttrium, YBCO [11] and from Y_2O_3 [21]. This ratio for YBCO was found to be approximately an order of magnitude higher than for oxygen-covered yttrium or Y_2O_3 [11]. According to Okajima [21], for a large number of oxides the ratio of the intensity of MO^+ (metal oxide) to that of M^+ is given by $K(-\Delta H_f \cdot m_c)^z$, where K is a constant, ΔH_f is the heat of formation of the oxide, to be used as the binding energy, m_c is the mean mass of the oxide, z is the valence number of the metal atom in the oxide. Using the valence number of Y in YBCO as +3 just as that in Y_2O_3 [22] and assuming the value of K to be the same both for Y_2O_3 and YBCO, the binding energy of Y in YBCO (i.e. heat of formation of Y-O bonds in YBCO) was found to be much higher than in Y_2O_3 [11].

Again, this high binding energy of yttrium atom in the YBCO structure was found to be very much consistent with that obtained from another measurement, such as, ion scattering spectroscopy (ISS) studies for the Ar^+ ions, scattered from the surfaces of yttrium as well as from YBCO [11]. From the measurement of scattered ion energies in these two cases (for the same bombarding ion energy and the angle of incidence), the difference between the binding energies of Y atom in YBCO and in metal was estimated and was found to be in good agreement with that obtained from secondary ion spectra [11].

The gain in binding energy of Y-atom in the YBCO lattice may be connected with the occurrence of compressed electrostatic forces acting upon Y^{3+} ion by the

two oppositely placed negatively charged CuO_2 conduction layers confined between two dielectric BaO planes [11].

Cu-O BINDING SITUATION AND VALENCY STATES OF COPPER

Seo *et al.* [13] made static SIMS measurements on two types of $Y_1Ba_2Cu_3O_{7-x}$ films with difference in oxygen content to study the Cu-O binding situation of YBCO films, as has been revealed by the results of other experiments, like X-ray or neutron diffraction [23], high resolution transmission electron microscopy [24], X-ray photoelectron spectroscopy [25] etc., that the oxygen content strongly affects the structure and properties of YBCO compounds. It was also suggested there [23–25] that the CuO_5 polyhedra and CuO_4 square-planar units, as shown in Fig. 6, exist in the YBCO structure. The existence of such molecular units in the YBCO structure was found to be directly reflected in the negative SIMS spectra of such a structure [13], indicating the secondary emission of CuO_4^- and CuO_5^- molecular ions from the sample. This once again confirms the 'as such' emission of these units from the YBCO surface. Since in the above experiment, the bombarding ion current (5 nA) and the ion energy (0.5 keV) were both very low (as is normally used in static SIMS), destruction of such molecular units due to ion bombardment could be avoided, making thereby their detection in the spectra possible [13]. This fact was confirmed by the primary energy variation of the intensity of these molecular ions [13]. There it was found that the molecular ion intensity decreased with the increasing primary ion energy.

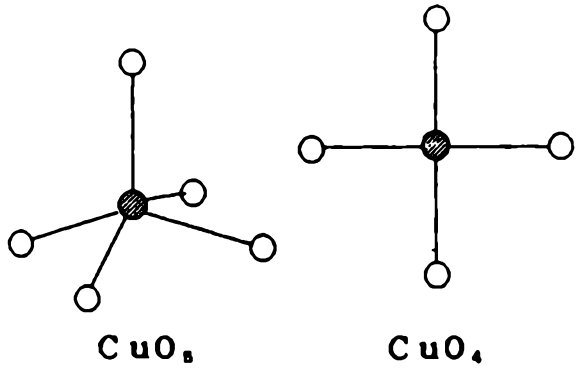

Fig. 6. The structure of CuO_4 and CuO_5 molecular units (after Seo *et al.* [13])

The YBCO films, deposited on MgO(100) substrates, were prepared by means of *rf* magnetron sputtering [13]. The oxygen content was measured to be 6.5 and 6.8, in the as-grown sample and in the same sample after getting annealed in sufficient oxygen flow, respectively. The static SIMS spectra of these two samples showed that the intensity of CuO_4^- and CuO_5^- secondary ions were relatively stronger for the sample with higher oxygen content (Fig. 7). This indicates that the Cu-O binding situation changes with the oxygen content of the YBCO structure, or in other words, Cu-O binding energy is more for a YBCO structures with higher oxygen

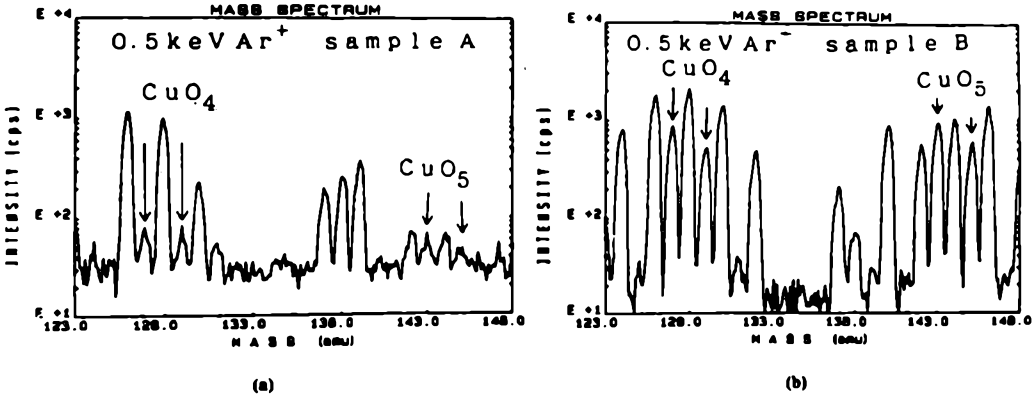

Fig. 7. Negative SIMS spectra of $Y_1Ba_2Cu_3O_{7-x}$ thin films: (a) sample A with oxygen content of 6.5, (b) sample B with oxygen content of 6.8 (after Seo *et al.* [13])

content. Also, it supports the hypothesis that CuO_4 and CuO_5 units do exist in the $Y_1Ba_2Cu_3O_{6.8}$ structure.

Depth analysis of these molecular ions was also carried out [13] for the two samples (with difference in oxygen content) where it was found that for the sample with higher oxygen content, intensity of these ions decreased with depth (Fig. 8). For the other sample, intensity of molecular ions was negligibly small and could hardly be detected as depth increased. Although these results support the YBCO structure with gradually less and less concentration as the depth increases, it cannot however be confirmed as the erosion of sputtering always accompanies the destruction of lattice [26].

The stoichiometry of YBCO compound implies that in an ionic description, one Cu^{3+} and two Cu^{2+} per formula unit are required to preserve charge-neutrality. However, it is important to ascertain the actual valence states of copper and/or of oxygen, needed to explain the formal valency 2.33 of copper in $Y_1Ba_2Cu_3O_7$. One possibility is to assume the usual O^{2-} and Cu^{2+} in Cu–O–Cu chains in the basal planes and a mixture of Cu^{2+} and Cu^{3+} in the CuO_2 conduction planes. In fact, to decide whether the hole (+ve charge) resides on copper (Cu^{3+}) or on oxygen O^{2-}, various theoretical and experimental approaches have been reported. Band structure calculations [27–29] and X-ray photoelectron spectroscopy studies [30–31] reveal mostly the presence of hybridization of Cu–3d and O–2p bands ($pd\sigma$ of CuO_2) around the Fermi energy along with the metallic behaviour of copper. Understanding of bonding and valence states of individual species is, therefore, needed for a thorough understanding of conduction and pairing mechanism.

Rajasekar *et al.* have recently made SIMS measurements of YBCO, CuO and mixtures of CuO and Cu_2O to investigate the valency as well as the bonding states of Cu in YBCO [14]. They explained the emission of Cu^+ from the YBCO structure to be essentially from the Cu–O–Cu chains. It was argued that this emission is due to the reduction of copper charge state (from Cu^{2+} to Cu^+) in the Cu–O–Cu chains,

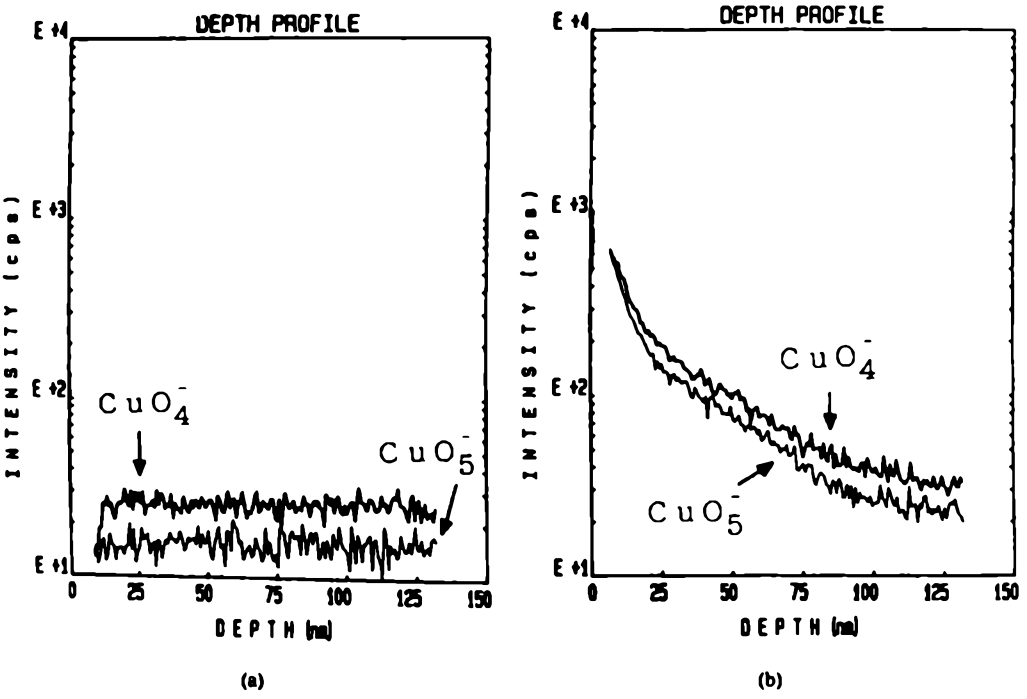

Fig. 8. The in-depth profiles of CuO_4^- and CuO_5^- secondary ions of $Y_1Ba_2Cu_3O_{7-x}$: (a) sample A, (b) sample B (after Seo *et al.* [13])

caused by the emission of labile oxygen (with higher emission cross section) due to the primary ion bombardment on the same chain [14]. The CuO_2 conduction plane has copper either in Cu^{3+} or Cu^{2+} state which rules out the emission of Cu^+ from this plane. Cu^{2+}, being quite stable in CuO_2 unit, cannot get reduced to Cu^+ in the same unit. The emission of Cu^{2+} is obviously from the CuO_2 plane, as was explained to be due to the reduction of Cu^{3+} to Cu^{2+} in the same plane by the removal of positive holes from the same plane. This removal of holes is caused as a result of the liberation of labile oxygen from the basal plane. The absence of Cu^{3+} in the SIMS spectrum [14] in case of YBCO confirms the above fact. This was also confirmed by XPS, ESCA and EPMA studies made by other workers in case of YBCO structure, where also the incident probing source with fairly high energy causes the removal of labile oxygen from the basal planes, leading to the conversion of Cu^{3+} to Cu^{2+} in CuO_2 unit of YBCO.

The relative intensity of Cu^{3+} to Cu^{2+} in case of YBCO [14] showed the emission of Cu^+ to be more than that of Cu^{2+}. This confirms the fact that the Cu–O bonding in CuO_2 unit is stronger giving rise to the less emission of Cu^{2+}. The high bond energy of Cu–O in CuO_2 units was explained as follows [14]. The Y-plane

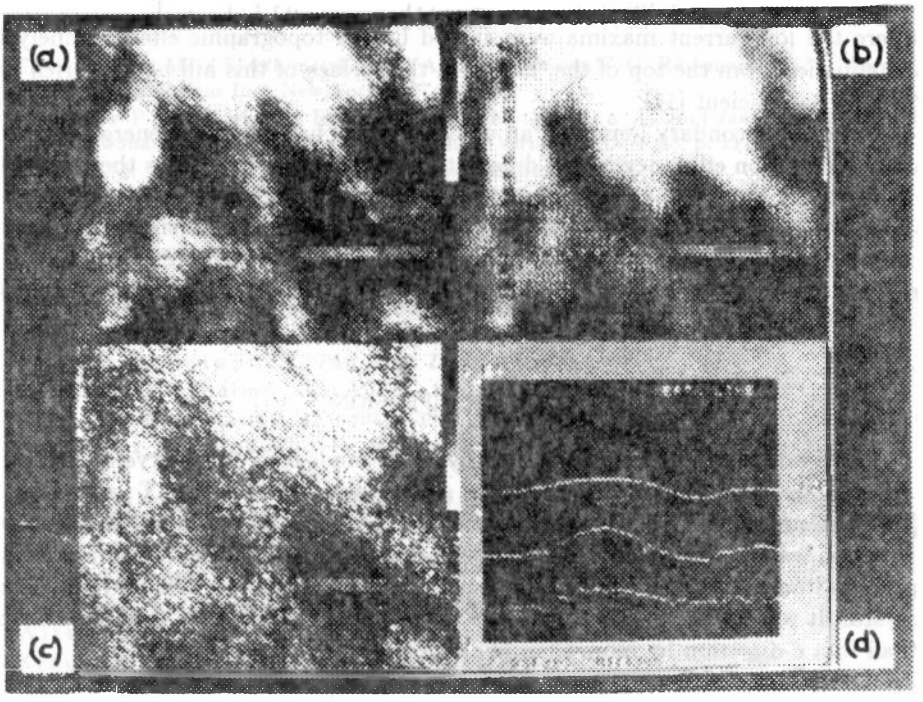

Fig. 9. Two-D images of the surface of $Y_1Ba_2Cu_3O_{7-x}$ in secondary ions Y^+ (a), Ba^+ (b) and Cu^+ (c). Distribution of secondary ion currents (d) Ba^+ (upper curve), Y^+, Cu^+ along vertical line (down) (after Chenakin [11])

is having a net positive charge, since each yttrium ion exists in Y^{3+} state in the YBCO structure. Therefore, the oxygen ions in the neighbouring CuO_2 units tend to balance this positive charge giving rise to the puckering of Cu–O–Cu bonds, as can be seen in Fig. 2, making thereby their bond energy increase.

SURFACE FEATURES

Two dimensional SIMS imaging of the surface of $Y_1Ba_2Cu_3O_{7-x}$ was taken in $^{89}Y^+$, $^{138}Ba^+$ and $^{65}Cu^+$ secondary ions [11], as shown in Fig. 9. One can see highly non-uniform lateral ion intensity distribution on the YBCO surface. The bright and dark regions correspond in general to each other in the different elemental images, yet do not coincide completely. Line scans across prominent features also show large variations in the secondary ion intensity for Y^+, Ba^+ and Cu^+ (Fig. 9d), which can be caused in general by the superposition of concentrational, topographic, matrix and chromatic contrasts of the YBCO surface. A SEM (scanning electron microscopy) study of the YBCO surface revealed that the surface is highly uneven with a sponge-like structure. Such topography of the YBCO surface has been

reflected in the vertical line scan (Fig. 9d) of the secondary ion current distributions, where the ion current maxima were caused by the topographic effect, namely by ion emission from the top of the 'hill' with the surface of this hill being Y-rich and O- and Ba-deficient [11].

Since the secondary ions from an uneven surface have different energy distributions, extraction efficiency is also different for these ions. This causes the chromatic contrast. An analysis of the horizontal line scan drawn across the large black spot (Fig. 9) which is certainly related to a deep hollow has revealed a significant contribution of chromatic effects to the topographic contrast, which are connected with reduced collection efficiency for highly energetic Y^+ ions emitted from the bottom area of the hollow.

OXYGEN DIFFUSION

Observation of ^{18}O tracer diffusion by SIMS made on a single crystal of YBCO with an array of steps on the stairlike surface was reported by Tsukui *et al.* [32]. The unique distribution of the diffused ^{18}O in the ab-plane and in the c-axis direction was shown visually as a mapped image, which revealed some fundamental processes on the oxygen penetration through the surface and diffusion in the inner crystal. It was found that at 530°C, the diffusion coefficient in an ab-plane is larger than in a c-direction by more than five orders of magnitude.

CONCLUSIONS

The recent various SIMS investigations of high-T_c superconducting compounds have been discussed. These studies have essentially proven to be able so as to shed some light on the aspects such as, nature and origin of impurities in the samples, copper-oxygen binding situation, high binding energies of Y and Er atoms in $Y_1Ba_2Cu_3O_{7-x}$ and $ErBa_2Cu_3O_{7-x}$ lattices, respectively, precise monitoring of deposition process form the preparation of superconducting thin films, bonding and valence states of copper, etc. Secondary emission of various components can directly be related in terms of the structural features. For example, the emission of CuO_4^-, CuO_5^- etc. from the YBCO surface indicates the presence of those units as building blocks inside the same structure. The secondary ion imaging of various emitted species has enabled us in mapping the lateral elemental distribution across the HTSC surfaces. Although, the existing studies, reported so far in this area, seem to be quite insufficient for better understanding of the various aspects of high-T_c superconducting materials, it is believed that in complementary to the other surface analytical techniques, SIMS will obviously give more and more fruitful information in this perspective.

REFERENCES

[1] *Secondary Ion Mass Spectrometry*, (eds.) A. Benninghoven, F. G. Rüdenauer, H. W. Werner, John Wiley and Sons Inc., New York 1987.

[2] Steffens P., Niehuis E., Rriese T., Benninghoven A., [in:] *Ion Formation from Organic Solids*, (ed.) A. Benninghoven, Springer-Verlag, Berlin 1983, p. 111.

[3] Castro M. E., Russel D. H., *Anal. Chem.*, 56 (1984), 578.

[4] Bednorz J. G., Müller K. A., *Z. Phys.*, B64 (1986), 189.

[5] [In:] *Strong Correlation and Superconductivity*, (eds.) H. Fukuyama, S. Maekawa, A. P. Malozemoff, Springer-Verlag, Berlin 1989.

[6] Shamma F. A., Fuggle J. C., *Physica*, C169 (1990), 325.

[7] Kurmaev E. Z., Finkelstein L. D., *Int. J. Mod. Phys.*, B5 (1991), 1097.

[8] Batlogg B., *Proc. LT-19.* Part III, *Physica*, B (1990).

[9] Allen G. C., Brown I. T., *Phil. Mag. Lett.*, 58 (1988), 219.

[10] Palatnik L. S., Klimovskii Yu. A., *Sov. Phys. Tech. Phys.*, 34 (1989), 369.

[11] Chenakin S. P., *Vaccum*, 42 (1991), 139.

[12] Rajasekar P., Chakraborty P., Ray N., Dey S. D., De Udayan, *Vacuum*, 43 (1992), 215.

[13] Seo S., Chang J. C., Matsui M., Takami H., *Jap. J. Appl. Phys.*, 28 (1989), L 994.

[14] Rajasekar P., Chakraborty P., Ray N., Dey S. D., Bandyopadhyay S. K., Barat P., De Udayan, *J. Appl. Phys.*, 73 (1993), 2429.

[15] De Udayan, Bhattacharyya T. K., Barua A. K., *Proc. Int. Conf. on Superconductivity*, Indian Institute of Science, Bangalore (India) 1990, 231.

[16] Wittmaack K., *Surf. Sci.*, 89 (1979), 668.

[17] Krauss A. R., Gruen D. N., *Surf. Sci.*, 92 (1980), 14.

[18] Krauss A. R., Gruen D. N., *Nucl. Instrum. Meth.*, 149 (1978), 547.

[19] Kosyachkov A. A., *Nucl. Instrum. Meth. Phys. Res.*, B65 (1992), 546.

[20] Cherepin V. T., Kosyachkov A. A., Vasilyev M. A., *Phys. Stat. Sol.*, A50 (1978), K 113.

[21] Okajima Y., *J. Appl. Phys.*, 55 (1984), 230.

[22] Sawyer D. T., *J. Phys. Chem.*, 92 (1988), 8.

[23] Fjellvag H., Karen P., Kjekshers A., Grepstad J. K., *Sol. State. Commun.*, 64 (1987), 917.

[24] Takayama-Muromachi E., Uchida Y., Matsui Y., Kato K., *Jap. J. Appl. Phys.*, 26 (1987), L 619.

[25] Watanabe H., Ikeda K., Miki H., Ishida K., *Jap. J. Appl. Phys.*, 27 (1988), L 783.

[26] Zalm P. C., *Surf. and Interface Analysis*, 11 (1988), 1.

[27] Mattheiss L. F., Hamann D. R., *Solid State. Commun.*, 63 (1987), 395.

[28] Massida S., Yu J., Freeman A. J., Koelling D. D., *Phys. Lett.*, A122 (1987), 198.

[29] Yu J., Massida S., Freeman A. J., Koelling D. D., *Phys. Lett.*, A122 (1987), 203.

[30] Steiner P., Konsinger V., Sander I., Siegwart B., Hufner S., Politis C., Hoppe R., Muller H. P., *Z. Phys.*, B67 (1987), 497.

[31] Arko A. J., List R. S., Fisk Z., Cheong S.-W., Thompson J. D., O'Rourke J. A., Olson C. G., Yand A.-B., Pi T.-W., Schirber J. E., Shinn N. D., *J. Magn. Magn. Matter.*, 75 (1988), L1.

[32] Tsukui S., Yamamoto T., Adachi M., Shono Y., Kawabata K., Fukuoka N., Nakanishi S., Yanase A., Yoshioka Y., *Jap. J. Appl. Phys.*, 30 (1991), L 973.